Taylor & Francis
Taylor & Francis Group

ORIGINAL RESEARCH

🔓 OPEN ACCESS Check for updates

Novel mRNA adjuvant ImmunER enhances prostate cancer tumor-associated antigen mRNA therapy via augmenting T cell activity

Zhen Xu[a]*, Ze-Xiu Xiao[b]*, Jing Wang[b]*, Hao-Wei Qiu[c], Fei Cao[a], Shi-Qiang Zhang[a], Yuan-Dong Xu[a], Han-Qi Lei[a], Heng Xia[c], Yun-Ru He[c], Gao-Feng Zha[b,c], and Jun Pang [ID][a]

[a]Department of Urology, Pelvic Floor Disorders Center, The Seventh Affiliated Hospital, Sun Yat-sen University, Shenzhen, Guangdong, China; [b]Drug Discovery Center, Shenzhen MagicRNA Biotech, Shenzhen, Guangdong, China; [c]Scientific Research Center, The Seventh Affiliated Hospital, Sun Yat-sen University, Shenzhen, Guangdong, China

ABSTRACT

Prostate cancer (PCa) is characterized as a "cold tumor" with limited immune responses, rendering the tumor resistant to immune checkpoint inhibitors (ICI). Therapeutic messenger RNA (mRNA) vaccines have emerged as a promising strategy to overcome this challenge by enhancing immune reactivity and significantly boosting anti-tumor efficacy. In our study, we synthesized Tetra, an mRNA vaccine mixed with multiple tumor-associated antigens, and ImmunER, an immune-enhancing adjuvant, aiming to induce potent anti-tumor immunity. ImmunER exhibited the capacity to promote dendritic cells (DCs) maturation, enhance DCs migration, and improve antigen presentation at both cellular and animal levels. Moreover, Tetra, in combination with ImmunER, induced a transformation of bone marrow-derived dendritic cells (BMDCs) to cDC1-CCL22 and up-regulated the JAK-STAT1 pathway, promoting the release of IL-12, TNF-α, and other cytokines. This cascade led to enhanced proliferation and activation of T cells, resulting in effective killing of tumor cells. In vivo experiments further revealed that Tetra + ImmunER increased CD8$^+$T cell infiltration and activation in RM-1-PSMA tumor tissues. In summary, our findings underscore the promising potential of the integrated Tetra and ImmunER mRNA-LNP therapy for robust anti-tumor immunity in PCa.

Introduction

Prostate cancer (PCa) stands out as the most prevalent malignant tumor in men.[1] Androgen deprivation therapy (ADT) serves as the first-line treatment for PCa. However, patients with advanced PCa inevitably progress to the castration-resistant prostate cancer (CRPC) stage, rendering them unresponsive to ADT.[2] Thus, the development of new therapeutic strategies for CRPC is urgently required.

Tumor-associated antigens (TAAs) exhibit elevated expression in tumor tissues while being minimally detectable in normal tissues.[3] Previous studies demonstrated that prostate-specific membrane antigen (PSMA), prostate acid phosphatase (PAP), and prostate stem cell antigen (PSCA) are PCa TAAs and promising candidates for therapeutic targets.[4–6] Transglutaminase 4 (TGM4) is highly expressed in PCa luminal epithelial cells but is rarely detected in extraprostatic tissues, and the immunogenicity of TGM4 had been reported in a previous study.[7] TAA messenger RNA (mRNA)-lipid nanoparticle (LNP)-based tumor therapy involves the adaptation of dendritic cells (DCs) followed by the initiation of T cell anti-tumor responses.[8] The processing of TAAs or neoantigens by DCs or other APCs is the foundation of anti-tumor responses to mRNA-based cancer therapeutics. DCs play a crucial role in antigen presentation and the induction of T cell-mediated immune responses.[9] TAA mRNA-LNPs administration initiates both specific humoral responses and cellular immune responses. DCs capture the TAA mRNA-LNPs, translate the targeted antigen, and process and present the antigen peptides to T cells to induce specific cytotoxicity to the relevant tumor.[10] However, central and peripheral tolerance to TAAs, which are non-mutated self-antigens, is characterized by weak immunogenicity. Thus, mRNA sequences must be optimized or combined with adjuvants or the drug delivery system must be modified to improve TAA-based mRNA therapeutics.[11]

T lymphocyte activation requires the stimulation of T cell receptors and costimulatory signals. DCs are a professional subset of APCs; after antigen processing, augmented DCs home to secondary lymphoid nodes and interact with T cells.[12] Immune cell homing is mediated by adhesion factors, chemokines, and chemokine receptors.[13] CCR7 is necessary for directional DCs homing and CCL19 and CCL21 are CCR7 ligands. Mobilized DCs migrate to multiple tissues, including tumor sites, and these chemokines facilitate the communication between DCs and T cells.[13,14] Costimulatory signals regulate T cell activation; T cell enhancement helps us fight against tumors or microbe infections, and T cell suppression
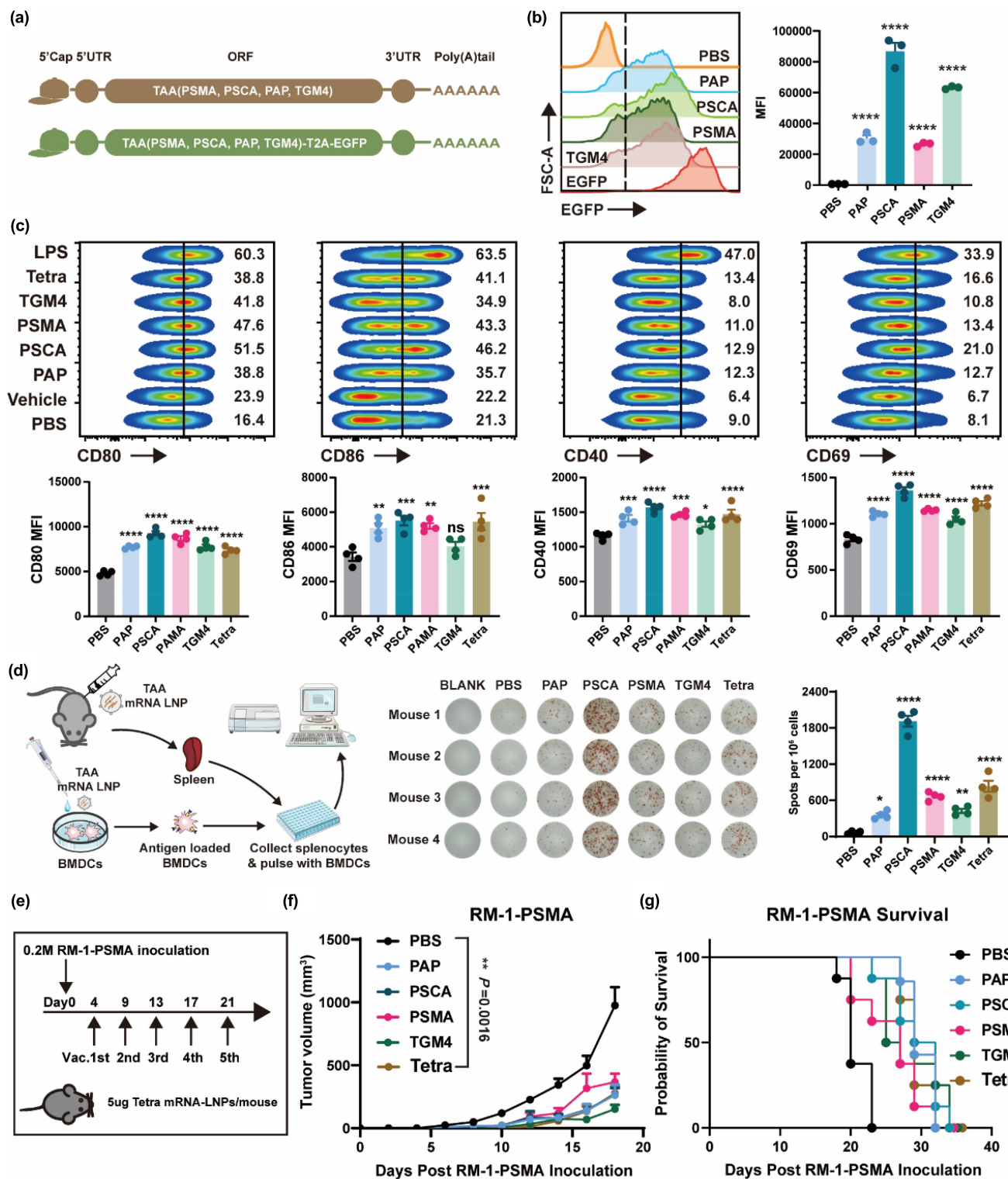
Figure 1. PCa TAA mRNA-LNPs-stimulated immunity suppresses prostate tumor growth in mice. (a) Schematic structure of TAA and TAA-EGFP mRNAs. TAA-EGFP mRNA was employed to verify mRNA expression efficiency; TAA mRNA was used for both in vitro and in vivo immunological assessments. (b) HEK293 cells were transfected with 1 μg of TAA-EGFP mRNA-LNPs and fluorescence intensity was detected by flow cytometry to verify mRNA expression 24 h after transfection. (c) BMDC maturation and activation levels after different treatments in vitro. Each symbol represented the BMDCs from one mouse transfected with 0.5 μg/ml mRNA-LNP. (d) IFN-γ ELISpot assays were used to detect the release of IFN-γ by spleen cells activated by BMDCs membrane antigens on day 5 after the last TAA mRNA therapeutic treatment in mice. Each dot represented one independent mice. (e) C57BL/6 mice ($n = 8$) were grafted with 2×10^5 RM-1-PSMA tumor cells and treated with different mRNA therapeutics by intramuscular injection on days 4, 9, 13, 17, and 21. (f and g) Tumor growth (f) and survival (g) of the tumor-bearing mice were observed until all mice died. Data were presented as means ± SEMs. Statistical significance was determined by One-Way ANOVA (b to d), Students t test (f), and Kaplan-Meier survival analysis (g). *$P < .05$, **$P < .01$, ***$P < .001$, and ****$P < .0001$.

helps us resist autoimmunity. After stimulation of antigen-manufactured APCs, the expression of 4-1BB (CD137/ILA/TNFRSF9) is inducible on T cells. The 4-1BBL-4-1BB pathway is involved in sustained activation, proliferation, differentiation, and effector function of T cells. Furthermore, 4-1BB signaling is preferentially involved in CD8⁺ T cell effector
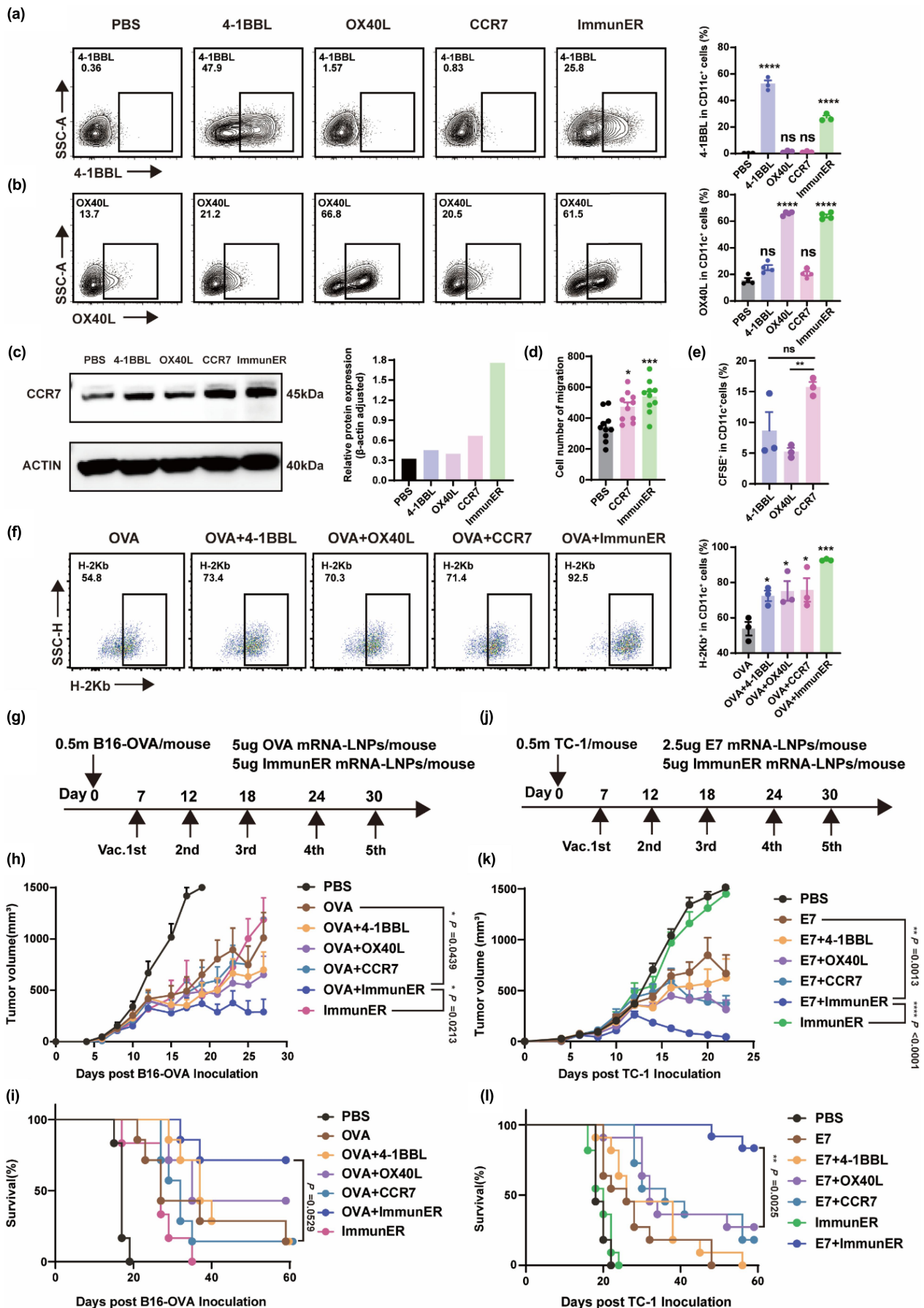
Figure 2. ImmunER enhances the function of dendritic cells and suppresses tumor growth. (a and b) The expression of 4-1BBL (a) and OX40L (b) mRNA on the cell membranes of BMDCs. Each symbol represented BMDCs from one mouse transfected with 0.5 μg/ml mRNA-LNPs. (c) BMDCs were transfected with 0.5 μg/ml mRNA-LNPs

function rather than CD4$^+$ T cell effector function.[15] OX40 is transiently expressed by T cells and down-regulated after T cell activation. The ligation of OX40L mediates the survival and expansion of both CD8$^+$ T cells and CD4$^+$ T cells.[16] Currently, mRNA therapies based on costimulatory molecules are undergoing clinical trials.[17,18]

We hypothesized that TAAs could initiate specific tumor cytotoxicity and that immunomodulatory factors could enhance the tumor-killing ability of T cells. Consequently, combining TAAs and immune factors might lead to more effective tumor clearance. In this study, we selected PSCA, PAP, PSMA, and TGM4 as candidate targets of TAA, used 4-1BBL, OX40L and CCR7 as immune-enhancing adjuvants. We explored their potential ability to inhibit tumor proliferation. We demonstrate that the four TAA mRNA-LNPs (referred to as Tetra) prime specific immunogenicity and the three immune enhancer mRNA-LNPs (referred to as ImmunER) enhance the immune reaction, resulting in the amelioration of tumor growth and prolongation of survival in a murine homograft cancer model. Moreover, the safety of the combined mRNA-LNPs was verified. Our study supports the feasibility of combining ImmunER and Tetra therapeutics to treat PCa. Furthermore, this new treatment concept may apply to other tumor types.

Materials and methods

Ethics statement

The IACUC Board at Shenzhen Bay Laboratory approved all animal procedures (AEZGF202201). All animal experiments were performed under pathogen-free conditions and in compliance with the Laboratory Animals Care and Use Guidelines set by the National Institute of Health.

Cell lines and animals

The RM-1 cell line was purchased from the American Type Culture Collection (ATCC). DC2.4, B16-OVA, HEK293, 293T, and TC-1 cell lines were purchased from Pricella company. The RM-1-PSMA cell lines were established by our group.

The 6–8-week-old C57BL/6 mice were purchased from Gempharmatech. The subcutaneous tumor cell transplant mouse models, including TC-1, B16-OVA, and RM-1-PSMA, were used in efficacy experiments. Each treatment group included at least 6 mice (and up to 12). Mice were randomly assigned to different groups before treatment. For each experiment, one researcher was responsible for drug administration, and another researcher was responsible for tumor measurement. For the in-situ prostate cancer model, subcutaneous

RM-1-PSMA tumors were excised on day 10 and cut into 1 mm^3 tissue blocks. Each RM-1-PSMA tissue block was then implanted into the anterior lobe of the prostate in mice using a 1 mL syringe needle. For the subcutaneous tumor model, tumor cells were subcutaneously injected in the right flank of the mouse. Subcutaneous tumor size was measured with a caliper every 2 to 3 days until the tumor volume reached the endpoint of 1500 mm^3. Tumor size was calculated using the formula (length×width^2/2. Mice were euthanized if they lost ≥ 20% of their body weight, were unable to eat, or had tumors exceeding 1.5 cm^3.

RNA-LNPs preparation, LNPs characterization, and transfection efficiency of LNPs

The ionizable amino lipid (A1A3) synthesis and the complete methodology for mRNA-LNP synthesis has been thoroughly detailed in our earlier article.[19] PAP, PSCA, PSMA, TGM4 mRNA were mixed initially before the synthesis of Tetra. Similarly, 4-1BBL, OX40L, CCR7 mRNA were mixed initially before the synthesis of ImmunER. A Malvern NanoAnalyzer was used to detect the size, polydispersity index, and zeta potentials at room temperature. The RiboGreen RNA assay (Invitrogen) was used to measure nucleic acid encapsulation efficiency. Gel qualitative method (Charles River) was used to measure endotoxin levels in purified vaccine. 2×10^5 Hek293 cells were transfected with mRNA-LNPs for 24 h to check transfection efficiency using flow cytometry (Beckman CytoFLEX S).

BMDC activation and maturation assay

BMDCs were cultured in 10 cm dishes in dendritic cell medium as described in the literature.[20] In brief, half of the medium was replaced every two days. On day 6, immature DCs were collected and plated at 1×10^6/ml. The DCs were treated with 0.5 or 1 μg/ml of various mRNA-LNPs or PBS. After 24 h of co-incubation, BMDCs were collected, stained using flow antibody staining, and analyzed via flow cytometry.

Statistical analysis

GraphPad Prism 9.3 was used to perform statistical analysis. An Agostino-Pearson test was performed to assess normality before analysis. When comparing two groups or more, two-sided Student's t tests with Welch corrections or one-way analysis of variance (ANOVA) with Tukey correction were performed. Kaplan-Meier survival analyses were performed, and p values were calculated using the log-rank test (Mantel-

and harvested for Western blot analysis. (d) DC2.4 migration ability after treatment with 0.5 μg/ml CCR7 mRNA-LNPs and ImmunER for 24 h was confirmed with Transwell migration assays. Results were calculated from two biological repeats in five technical duplicates. (e) In vivo BMDCs migration assay (n = 3). (f) The antigen uptake and presentation abilities of BMDCs were evaluated by flow cytometry. Each symbol represented BMDCs from a separate mouse transfected with 20 μg/ml OVA peptide. (g) Mice (n = 6–7) were grafted with 5 × 10^5 B16-OVA tumor cells and treated with different mRNA therapeutics by intramuscular injection on days 7, 12, 18, 24, and 30. Tumor growth curve (h) and survival (i) of B16-OVA tumor-bearing mice after intramuscular injection with PBS, OVA, OVA + 4-1BBL, OVA + OX40L, OVA + CCR7, ImmunER and OVA + ImmunER mRNA therapeutics, respectively. (j) Mice (n = 11–12) were grafted with 5 × 10^5 TC-1 tumor cells and treated with different mRNA therapeutics by intramuscular injection on days 7, 12, 18, 24, and 30. Tumor growth curve (k) and survival (l) of TC-1 tumor-bearing mice after intramuscular injection with PBS, E7, E7 + 4-1BBL, E7 + OX40L, E7 + CCR7, ImmunER and E7 + ImmunER mRNA therapeutics, respectively. Data were presented as means ± SEMs. Statistical significance was determined by One-Way ANOVA (a, b, d to f), Student t test (h, k), and Kaplan-Meier survival analysis (i, l). *P < .05, **P < .01, ***P < .001 and ****P < .0001.
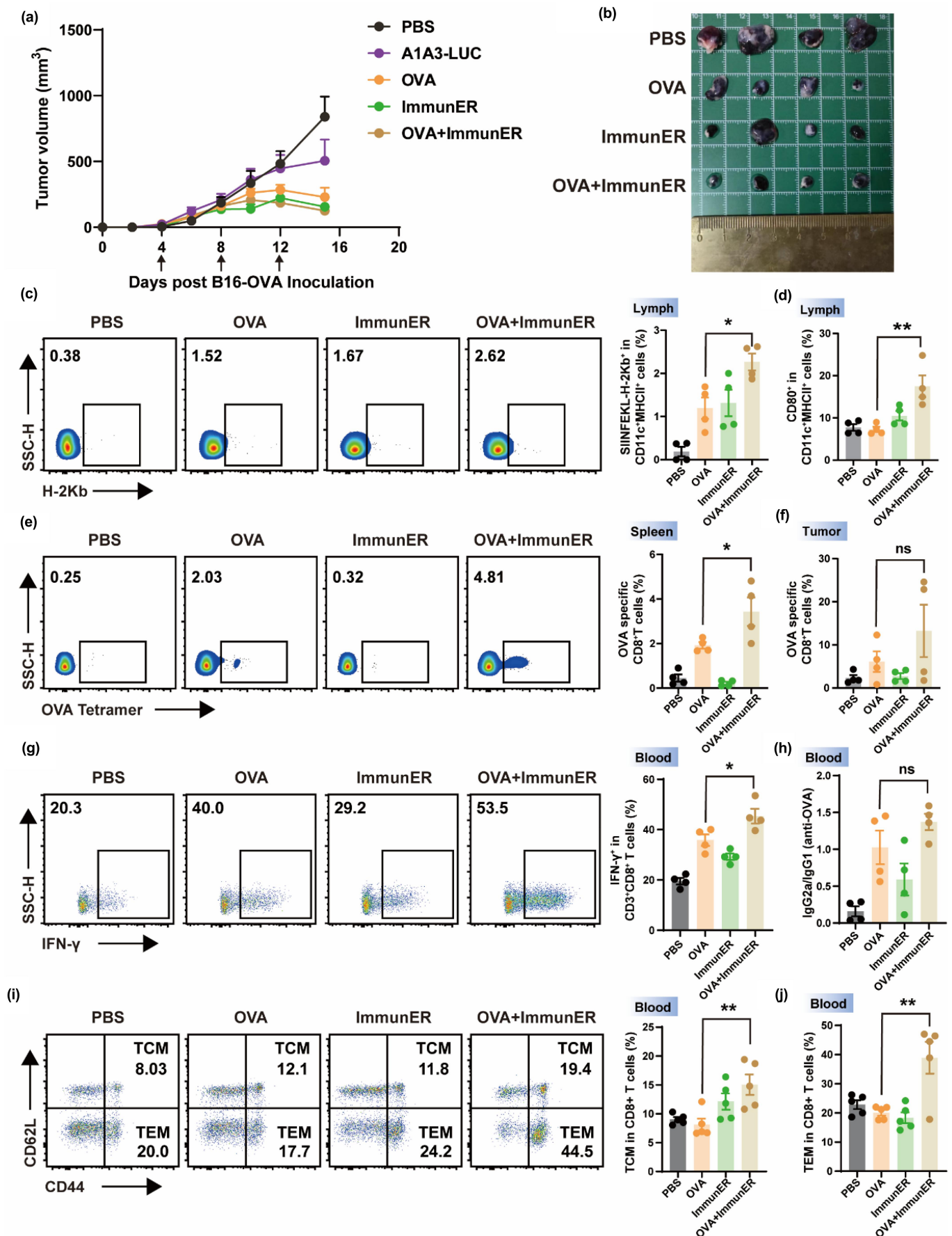
Figure 3. ImmunER enhances the level of immunity in vivo. C57BL/6 mice (n = 4) were grafted with 5×10^5 B16-OVA tumor cells and treated with PBS, luciferase, OVA, ImmunER, and OVA + ImmunER mRNA therapeutics on Day 4, 8, 12, respectively. (a) Tumor growth curve of B16-OVA tumor-bearing mice. (b) The tumors of each group were photographed 15 days after tumor inoculation. (c) SIINFEKL-H-2Kb+CD11c+MHC-II+ DCs in lymph nodes. (d) DCs maturation levels in lymph nodes. (e) OVA

Cox). Data are expressed as means ± SEMs. $p < .05$ was considered a significant difference.

Results

A1A3 LNPs passively target antigen presenting cells after intramuscular injection

In our previous research, we outlined the screening process and immunological assessment of A1A3 LNPs.[19] Nonetheless, the distribution of A1A3 LNPs within tumor-bearing mice remain unresolved. To address this gap, we conducted a comparative analysis between A1A3 LNPs and MC3 LNPs, a commercially available lipid, to evaluate the in vivo distribution of A1A3 LNPs. 5 µg Luciferase (LUC) mRNA-LNPs was injected intramuscularly when tumors reached 100 mm³ (Figure S1a). Six hours post-injection, whole-body imaging revealed that the fluorescence signal of A1A3 LUC mRNA-LNPs was 1.6 times stronger than that of MC3 LUC mRNA-LNPs (Figure S1b,c). Subsequent to a 24-hour interval, we euthanized the mice, dissected vital organs and tumors, and observed a robust luminescent signal in the lymph nodes, with little fluorescence signals detected in the tumors (Figure S1d,e).

To further explore the intracellular distribution of lipid nanoparticles, Green Fluorescent Protein (EGFP) mRNA was employed. The percentage of EGFP-positive DCs in the draining lymph nodes escalated to 10%. Moreover, the percentage of EGFP-positive natural killer (NK) cells surpassed 5% (Figure S1f and Figure S2a,b). Despite observing a higher percentage of EGFP-positive tumor cells in the A1A3 group, this percentage remained below 1% (Figure S1g). Immunohistochemistry conducted at the injection site revealed edema and immune cell infiltration in muscle tissue post-administration. Our observations indicate that immune cells infiltrating the muscle tissue can undergo transfection with A1A3 LNPs, leading to the expression of EGFP. However, the normal morphology of muscle tissue remained unchanged, and staining outcomes did not suggest overexpression of EGFP in the muscle tissue (Figure S1h).

Immunogenicity and treatment efficacy of PCa TAA mRNA-LNPs

PSMA, PSCA, PAP, and TGM4 are extensively expressed in prostate cancer tissue and are PCa-associated antigens.[4,7] Publicly available data demonstrated similar histological distributions of these TAAs in mice and humans (Figure S3a,b).[21] The expression of TAAs was further confirmed in RM-1-PSMA cell line, along with the corresponding subcutaneously transplanted tumors (Figure S4a, b). After the animal model was established, mRNA-LNPs was synthesized and its quality was controlled to ensure the reproducibility of results (Figure S5a-e). Furthermore, we assessed the cytotoxicity of

mRNA-LNPs on bone marrow-derived dendritic cells (BMDCs) via CCK8 and apoptosis assay, and the results showed that the synthetic mRNA-LNPs had no significant effect on DCs viability when the concentration was less than 1 µg/ml (Figure S6a – g). We synthesized the open reading frames of PSMA, PSCA, PAP, and TGM4 and synthesized the corresponding mRNAs (Figure 1a).The translation efficiency of mRNA was assessed using EGFP.[22] The translation efficiency of TAA-EGFP mRNA was assessed using the EGFP sequence inserted behind the TAA mRNA sequence, measured by flow cytometry on HEK293 cell lines (Figure 1a,b). DC maturation and activation are crucial to antigen presentation and subsequent immune responses. The four TAA mRNA-LNPs initiated the maturation (CD80 and CD86) and activation (CD40 and CD69) of BMDCs (Figure 1c and Figure S7a). A second exposure to the same antigen usually results in enhanced antigen-specific T-cell mediated immunity, which is referred to as recall immunity. After immunizing mice twice with the four TAA mRNA-LNPs, the splenocytes from C57BL/6 mice were isolated and subjected to ELISpot assays. The TAA mRNA-LNPs-pretreated DCs induced significantly more IFN-γ production compared with control DCs (PBS) (Figure 1d).

In a murine subcutaneously-implanted RM-1-PSMA tumor model, the four TAA mRNA-LNPs separately suppressed tumor development at an early stage. However, treatment with the combined TAAs did not substantially extend the median survival of tumor-burdened mice compared to the single TAA mRNA-LNPs treatments (Figure 1e–g). Considering tumor heterogeneity, the combination of TAAs could prove more advantageous for PCa patients, as the alliance of TAAs induces a broad spectrum of clinical application. Therefore, PCa TAA mRNA-LNPs (Tetra) was selected for subsequent studies. Subsequently, we performed animal experiments again and found that intramuscular injection of non-related mRNA-LNPs had minimal impact on the subcutaneous tumor growth of RM-1-PSMA (Figure S8a,b). Overall, our findings demonstrate that Tetra is capable of inducing antigen-specific cytotoxicity.

ImmunER facilitates anti-tumor efficacy

The 4-1BBL-4-1BB axis promotes the maintenance of anti-tumor immunity through the expression of 4-1BBL on antigen-presenting cells and receptors on T cells or NK cells.[15] The OX40L-OX40 pathway enhances the Th1-mediated immune response and promotes the generation and maintenance of memory CD8+T cells.[16] CCR7 plays a crucial function in the homing of DCs to lymphoid tissue. We synthesized mRNA for 4-1BBL, OX40L, and CCR7 and fabricated the corresponding mRNA-LNPs. Successful expression of mRNA-LNPs was observed in transfected target cells (Figure 2a–c and Figure S9a). We found that CCR7 mRNA-LNPs slightly promoted

specific CD8+T cells in spleen. (f) OVA specific CD8+T cells in tumor. (g) IFN-γ+CD8+T cells in blood. (h) Ratios of OVA specific IgG2a/IgG1. C57BL/6 mice (n = 5) were treated with PBS, OVA, ImmunER, and OVA + ImmunER mRNA therapeutics on day 0 and 5. Blood samples were collected 3 weeks after the last treatment. (i and j) Proportion of CD8+ TCM and TEM in blood. Data in a, c to j were presented as means ± SEMs. Statistical significance was determined by One-Way ANOVA (c to j). *P < .05, and **p < .01.
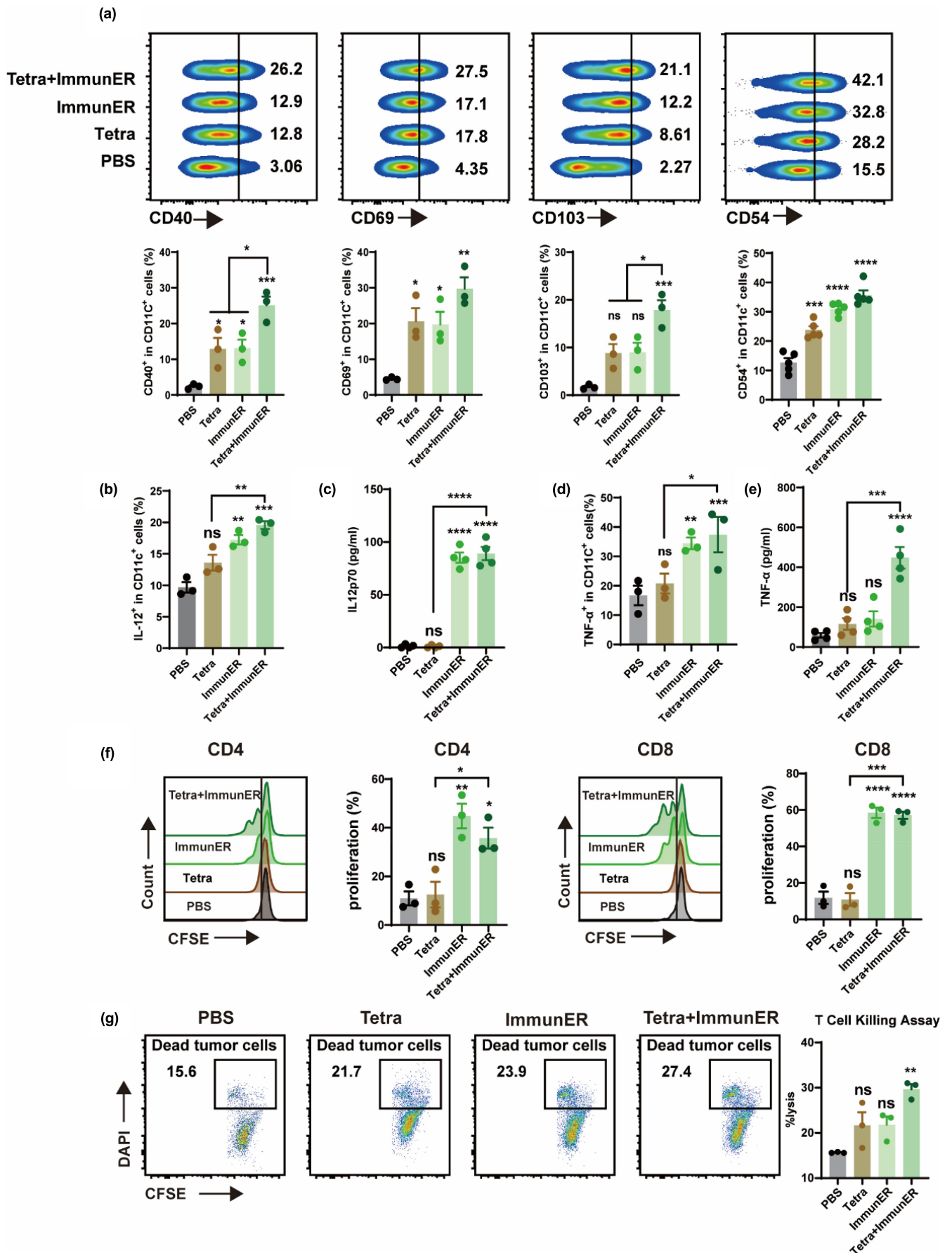
Figure 4. Tetra combined with ImmunER enhances the function of BMDCs in vitro. (a) Representative flow cytometry data and statistical analysis showing BMDCs activation induced by PBS, Tetra, ImmunER, and Tetra + ImmunER. Each symbol represented BMDCs from one mouse treated with 1 μg/ml mRNA-LNPs. (b and c) Flow

CCL21 release from BMDCs, which may drive peripheral DCs to lymph node metastasis in vivo (Figure S9B). Subsequently, we observed a notable upregulation in the migration of DCs both in vitro and in vivo upon the application of CCR7 mRNA-LNPs. (Figure 2d,e and Figure S9c,d). ImmunER, consisting of 4-1BBL, OX40L, and CCR7, also upregulated the expression of CD80, CD86, and MHC-II, indicating the maturation of DCs (Figure S9e). The dominant CD8 epitope of OVA peptide is SIINFEKL, which binds to MHC-I on DCs and can be detected as SIINFEKL-H-2Kb complexes. The formation of these complexes is indicative of the antigen-presenting ability of DCs. SIINFEKL-H-2Kb complexes increased in ImmunER-programed DCs (Figure 2f). These results demonstrate that ImmunER enhanced antigen presentation, and migration of DCs.

B16-OVA and TC-1 tumor models are well-established murine tumor models commonly used in cancer immunotherapy research. Unlike tumor-associated antigens, OVA and human papillomavirus E7 protein are known to efficiently initiate immune responses.[8,23] Therefore, we conducted experiments using two murine tumor models to investigate whether the combination of ImmunER and exogenous protein mRNA could enhance immunity (Figure 2g,j). In B16-OVA model, the groups treated with OVA + 4-1BBL, OVA + OX40L, and OVA + CCR7 conferred a moderate level of immune therapeutic effect. OVA + ImmunER immunized group maintained a high survival rate (Figure 2h,i). Similar results were observed in TC-1 model (Figure 2k,l). In the murine B16-OVA model, 2/7 mice treated with the OVA-conjugated ImmunER regimen achieved complete remission (CR) (Figure S10a). In the murine TC-1 model, treatment with E7 combined with ImmunER administration induced 83.3% (10/12) CR in the murine TC-1 tumor model (Figure S10b). These results demonstrate that ImmunER mRNA enhanced a universal anti-tumoral response in multiple murine tumor models. In addition, intramuscular administration of ImmunER inhibited tumor growth in mice subcutaneously implanted with RM-1-PSMA cells (Figure S10c). Taken together, our results indicated that ImmunER enhanced antigen presentation in DCs and anti-tumor efficacy.

ImmunER enhances antigen-specific T cell response and memory immune response in vivo

In this study, we employed the B16-OVA model to further elucidate the mechanism by which ImmunER enhances immunity. Following three injections, treatments with OVA, ImmunER, and OVA + ImmunER all demonstrated significant suppression of tumor growth (Figure 3a,b). Within lymph nodes, the presentation of epitopes to T cells by antigen-burdened DCs is essential for cytotoxic T cell priming.[13,14] The combined treatment group exhibited the highest number of SIINFEKL-H-2Kb^{+} DCs on the drainage side (Figure 3c). Besides, the proportion of CD80^{+} DCs in the draining lymph

nodes of the OVA + ImmunER group was twice compared to OVA or ImmunER alone (Figure 3d). Subsequent assessment of OVA-specific T cells revealed that the OVA + ImmunER group exhibited the highest proportion of OVA-specific T cells within both the spleen and tumor-infiltrating immune cells, with a statistically significant difference in spleen (Figure 3e,f). IFN-γ, playing a crucial role in tumor killing by specific T cells, showed a 15% increase in the proportion of IFN-γ-releasing T cells after ImmunER combined with OVA compared to OVA alone (Figure 3g). The serum OVA-specific IgG2a/IgG1 ratio was > 1.0 in the combination treatment group, further indicating that ImmunER played a role in promoting cellular immunity (Figure 3h). Overall, the above experiments demonstrate that ImmunER significantly enhanced antigen presentation and increased the proportion of antigen-specific T cells.

To assess whether ImmunER could augment vaccine protection, healthy mice were immunized on days 0 and 5. Three weeks after the last treatment, blood samples were collected to assess the levels of central memory T cells (TCM) and central effector T cells (TEM). The proportion of TCM and TEM in the blood of the combination group was twice that of the OVA group at 3 weeks after the last dose (Figure 3i,j), demonstrating that ImmunER enhanced the production of antigen-specific immune memory. Besides, we observed a marginal improvement in the outcome of B16-OVA-bearing mice with ImmunER alone. In an effort to elucidate this phenomenon, we conducted in vivo killing experiments. Our findings revealed that spleen cells from mice immunized with ImmunER exhibited a 30% cytotoxicity against OVA peptide-incubated spleen cells within 22 hours (Figure S10d).

ImmunER facilitates the immunity induced by Tetra in vitro

Tetra for PCa induces tumor-specific cytotoxicity, and ImmunER enhances the immune response. Therefore, we hypothesized that the combination of TAA and ImmunER would exert a greater suppressive effect on tumors. The expression of CD40 and CD69 indicates DC activation. CD103^{+}DCs play a role in cross-presentation of antigens to CD8^{+}T cells, and CD54 (ICAM-1) is critical in establishing the immune synapse.[24,25] The combination of Tetra and ImmunER enhanced the activation of DCs more effectively than Tetra or ImmunER separately (Figure 4a). Simultaneously, we observed an increase in IL-12 and TNF-α signals in flow cytometry and ELISA, with a statistically significant difference in the Tetra + ImmunER group compared with the Tetra group (Figure 4b-e). Additionally, the secretion and release of IL-6 and IFN-γ were enhanced in the Tetra + ImmunER group (Figure S11a). Pretreatment of DCs with Tetra +

---

cytometry analysis (b) and ELISA (c) showed the expression of IL-12 in BMDCs. (d and e) Flow cytometry analysis (d) and ELISA (e) showed the expression of TNF-α in BMDCs. (f) Representative histograms and statistical analysis showing T cell proliferation in vitro. (g) Representative flow cytometry data and statistical data showing the killing activity of splenic T cells 7 days after the last treatment. Data in a to g were presented as means ± SEMs. Statistical significance was determined by One-Way ANOVA (a to g). *P < .05, **P < .01, ***P < .001, and ****P < .0001.
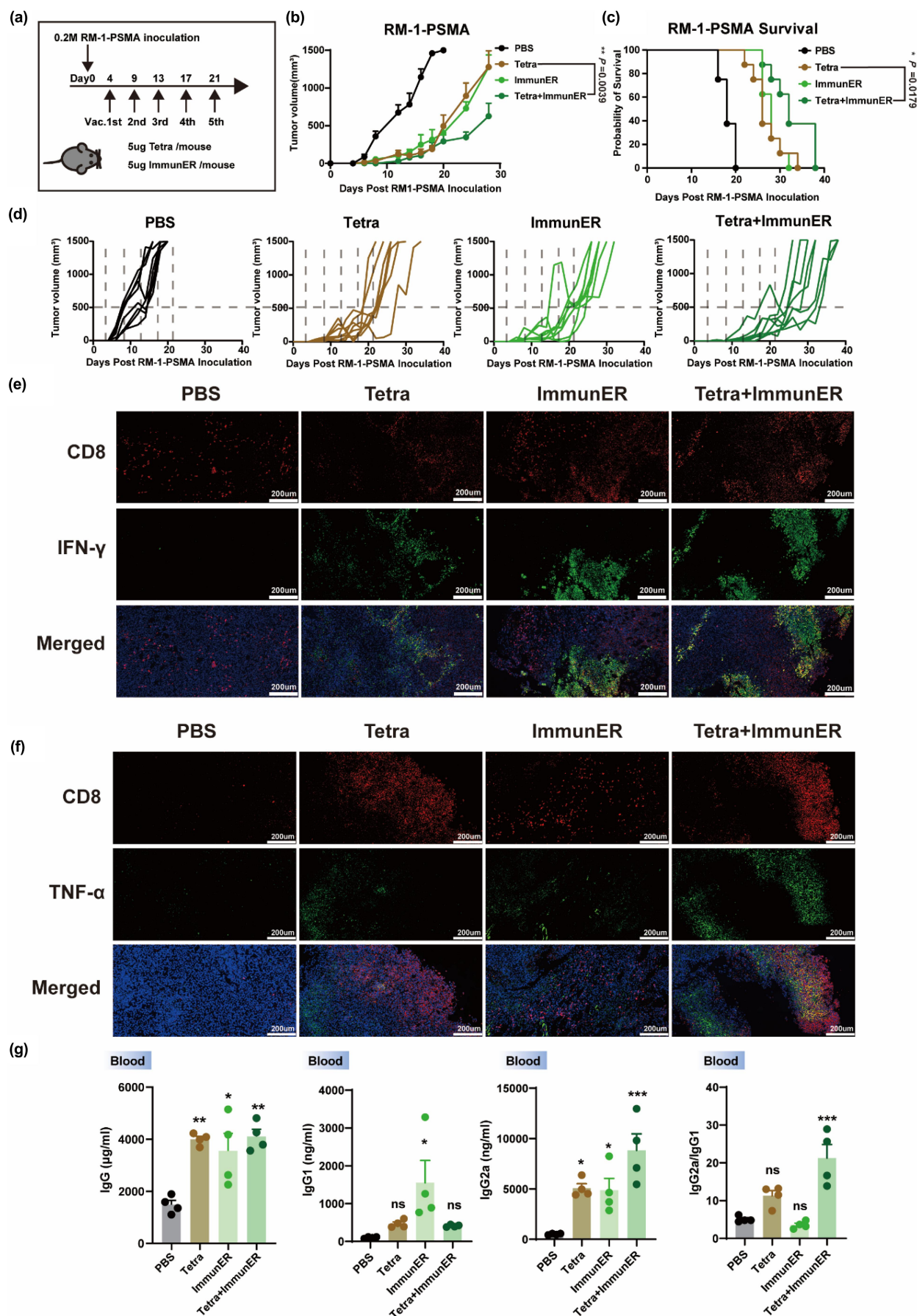
Figure 5. Tetra-ImmunER exhibits therapeutic effects and alters the tumor immune microenvironments in a PCa murine model. (a) C57BL/6 mice (n = 8) were grafted with 2×10^5 RM-1-PSMA tumor cells and treated with PBS, Tetra, ImmunER, and Tetra + ImmunER mRNA therapeutics on days 4, 9, 13, 17, and 21. Tumor size growth (b)

ImmunER also recalled abundant IFN-γ specific production of T cells (Figure S11b). TAA-programmed DCs stimulate the proliferation of T cells and prime T cells for specific tumor cytotoxicity.[4] Compared with Tetra alone, coupling Tetra with ImmunER effectively promoted T cell proliferation (Figure 4f). In addition, spleen cells from different treatment groups were harvested and incubated with tumor cells for 6 hours. The combination group exhibited the elimination of approximately 29% of the RM-1-PSMA tumor cells, while only about 22% of the tumor cells in the single treatment group were cleared. (Figure 4g and Figure S7d). Overall, Tetra initiates a specific anti-tumoral response and ImmunER boosts this response. Thus, the combination of Tetra and ImmunER displays greater anti-tumor efficacy than either agent alone.

Combination therapy inhibits mouse prostate cancer growth in vivo

The effectiveness of combination therapy with Tetra and ImmunER was also demonstrated in murine models of PCa. In the RM-1-PSMA subcutaneous allograft model, Tetra combined with ImmunER induced anti-tumoral effects (Figure 5a,b); Overall, there was a delay in tumor growth in response to the combination treatment, with 3 mice reaching the endpoint volume by day 38 after tumor grafting. Survival in the Tetra + ImmunER group was better than the Tetra regimen alone (Figure 5c,d). Monoclonal antibodies to CD8a successfully blocked all CD8+T cells in the mice's blood (Figure S12a, b). Notably, the depletion of CD8+T cells significantly impaired the anti-tumor efficacy of the Tetra + ImmunER combination therapy (Figure S12c). We further assessed the efficacy of combining mRNA therapy with ICI in the suppression of RM-1-PSMA subcutaneous tumors. During a 25-day observation period, two out of five mice in the Tetra + ImmunER + ICI group achieved CR, whereas all mice in the ICI monotherapy group met the criteria for sacrifice by day 25 (Figure S12d-f). The robust tumor suppression capability of the Tetra + ImmunER therapy was additionally demonstrated using the RM-1-PSMA orthotopic model (Figure S12g-h). Collectively, these animal experiments suggest that the Tetra + ImmunER therapy effectively suppresses PCa tumor growth and extends the survival of PCa-bearing C57BL/6 mice.

Immunofluorescence staining and flow cytometry data showed that IFN-γ and TNF-α increased at the tumor site in the combined treatment group, and the IFN-γ and TNF-α staining overlapped with CD8+ T cells (Figure 5e,f and Figure S11c-f), indicating that combination therapy with PCa Tetra and ImmunER enhanced the functional CD8+T cells response at the tumor site. The humoral immune response was also investigated. Total IgG, IgG1, and IgG2a levels were upregulated in the combination treatment group (Figure 5g). The ratio of IgG2a/IgG1, suggesting the Th1 type cellular immune response,[23] also increased in the combination therapy group. This part of the data is consistent with the change of OVA-specific IgG2a/IgG1 ratio in the B16-OVA model, suggesting that TAA combined with ImmunER suppressed the tumor primarily through cellular immunity.

The safety of combinational mRNA therapeutics was explored in vivo. Aspartate aminotransferase (AST), alanine aminotransferase (ALT), blood urea nitrogen (BUN), and creatinine (CREA) levels were measured to determine the effects of treatments on liver and renal functions. None of the treatments significantly affected liver or renal function (Figure S13a-d). Major organs were collected from mice in the control and treated groups and examined histologically. No significant toxicity was observed in any organ (Figure S14). These results demonstrate that repeated administration of combination therapy with Tetra and ImmunER did not induce any adverse effects in mice, confirming the short-term safety of the combination therapy.

Combination therapy reconstitutes the immunity characteristics in tumor-bearing mice

Effective anti-tumor responses require T cells capable of recognizing tumor antigens.[26] In our study, the accumulation of CD8+ T cells increased at the tumor site after combination treatment in RM-1-PSMA allograft mice (Figure 6a,b and Figure S11g). In general, when DCs upregulate 4-1BBL or OX40L, T cells should correspondingly up-regulate 4-1BB or OX40. The heightened infiltration of OX40+CD8+T cells and 4-1BB+CD8+T cells within tumors can impede tumor growth and enhance the outcome of mice.[15,16] Flow cytometry analysis revealed a significant increase in the proportion and expression intensity of OX40+CD8+T cells and 4-1BB+CD8+T cells among tumor-infiltrating T cells in the combined treatment group (Figure 6c,d). Furthermore, an elevated proportion of CD44+CD8+T cells was observed in the combined treatment group (with PBS) (Figure 6e). These results indicate that the combination therapy markedly promoted the activation of T cells. Myeloid-derived suppressor cells (MDSCs) infiltration typically increases in prostate tumor tissues, significantly inhibiting T cell activity.[27] Our data show that the combination of Tetra and ImmunER markedly reduced MDSCs infiltration within the tumors (Figure S11h). Besides, flow cytometry results indicated a slight increase in the proportion of Tregs among tumor-infiltrating lymphocytes following the combination treatment (Figure S11i).

In lymph tissues, TCM cells provide immune surveillance against known pathogens.[28] TCM cells were upregulated in the treatment group (Figure 6g,j). During the process of cell lysis, CD8+ effector T cells undergo fusion with the target cell membrane, and subsequently discharge cytotoxic mediators

---

and overall survival (c) of RM-1-PSMA-bearing mice treated with the indicated mRNA-LNPs therapeutic were shown. (d) Tumor growth curves were shown for individual animals. C57BL/6 mice (n = 5) were grafted with 2 × 10⁵ RM-1-PSMA tumor cells and treated with different mRNA therapeutics by intramuscular injection on days 4, 9, and 13. Mice were sacrificed on day 18 after tumor seeding. (e and f) Confocal fluorescence images of tumor tissues in the PBS, Tetra, ImmunER, and Tetra + ImmunER treatment groups. (e) The nuclei, CD8, and IFN-γ were stained with blue (DAPI), red, and green, respectively. (f) In consecutive sections, the nuclei, CD8, and TNF-α were stained with blue (DAPI), red, and green, respectively. (g) Total IgG, IgG1, IgG2a, and IgG2a/IgG1 levels in sera after treatment with PBS, Tetra, ImmunER, or Tetra + ImmunER. Data in b, g were presented as means ± SEMs. Statistical significance was determined by Student t test (b), Kaplan-Meier survival analysis (c) and One-Way ANOVA (g). *P < .05, **P < .01, and ****p < .0001.
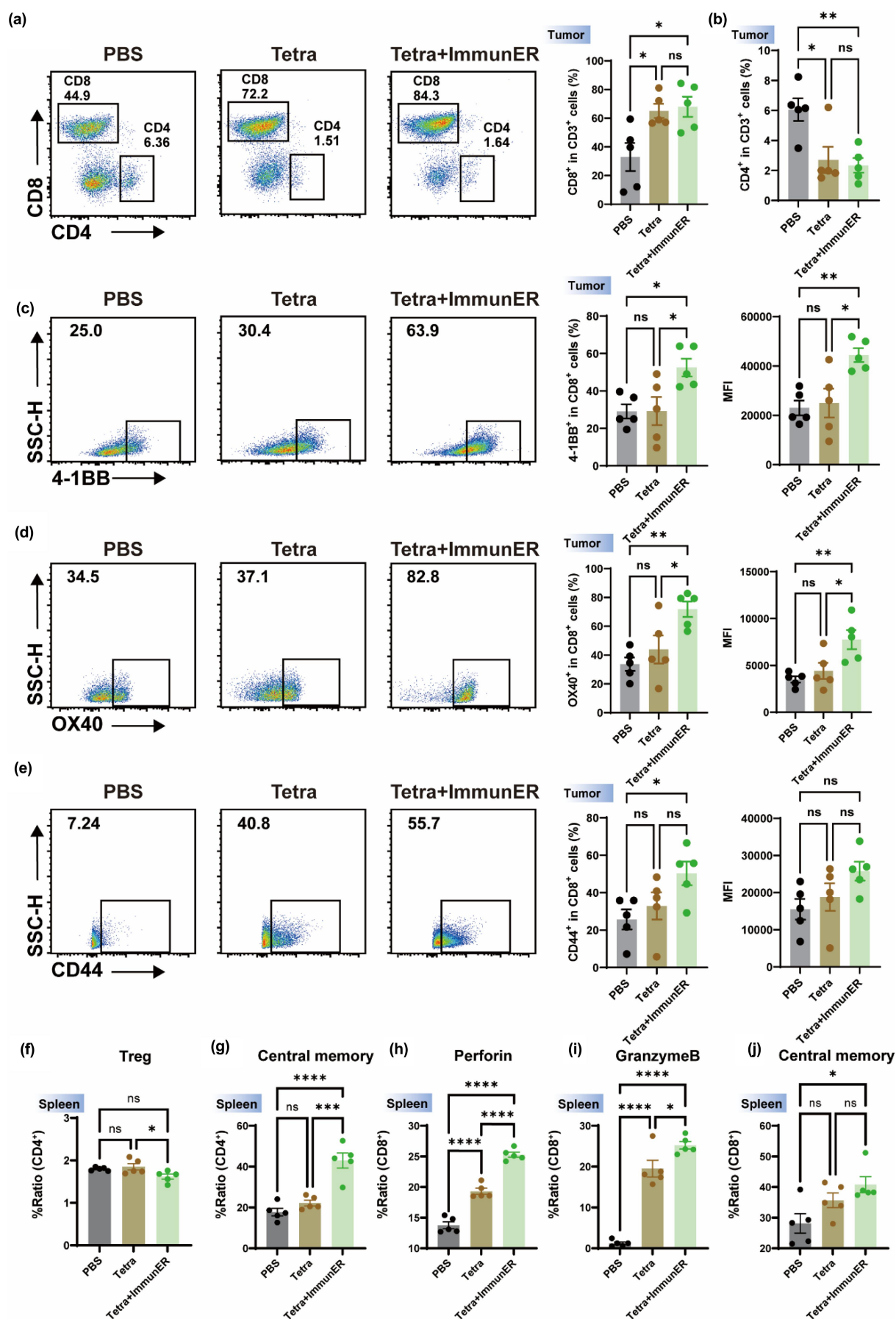
Figure 6. PCa Tetra-ImmunER upregulates cell adaptive immunity. C57BL/6 mice (n = 5) were grafted with 2×10^5 RM-1-PSMA tumor cells and treated with PBS, Tetra, and Tetra + ImmunER mRNA therapeutics on Day 4, 9, 13, respectively. Mice were sacrificed on day 18. (a and b) Representative flow dot plots and statistical analysis of

including perforin and granzyme.[29] In spleen, the ability of CD8$^+$ T cells to release both granzyme and perforin was enhanced in the treated group (Figure 6h,i). Interestingly, we observed a mildly reduced proportion of Tregs in the spleen (Figure 6f). These results demonstrate that combining Tetra with ImmunER enhances adaptive cytotoxicity to inhibit tumor growth and prolong the survival of mice with PCa.

Tetra combined with ImmunER reprograms transcription in BMDCs

To investigate the molecular basis of BMDC activation following treatment with various mRNA drugs, we collected BMDCs from four mice and treated the cells with different mRNA drugs for 24 hours. Transcriptome analysis was then performed using RNA sequencing. Principal component analysis demonstrated strong replication within clusters, and notable distinctions between the treatment and control groups (Figure 7a). The volcano plots visually show the differentially expressed genes. In BMDCs, 514 genes (426 up-regulate genes and 88 down-regulate genes) were differentially expressed in response to Tetra treatment compared with control treatment (Figure 7b,c), and 233 genes (170 up-regulate genes and 63 down-regulate genes) were differentially expressed in Tetra-treated BMDCs compared with Tetra + ImmunER-treated BMDCs (Figure 7b,d).

The Ccl22$^+$ cDC1 subset of DCs specifically correlates with the upregulation of TEM cells and a decrease in exhausted CD8 T cells.[30] Accordingly, our DC cluster analysis revealed that mRNA from BMDCs treated with Tetra and ImmunER developed cDC1-Ccl22 reprogramming (Figure 7e), which was confirmed by RT-qPCR (Figure 7f). KEGG enrichment analysis and GSEA-KEGG analysis suggested that pathways involved in innate and adaptive immunity were highly activated in BMDCs treated with Tetra + ImmunER compared to BMDCs treated with Tetra (Figure 7g,h). The JAK-STAT pathway, known for its involvement in cytokine and growth factor production as well as T cell priming of DCs,[31] was notably up-regulated in BMDCs treated with Tetra and ImmunER (Figure 7i). The increased level of STAT1 phosphorylation at Ser727 further substantiated this activation (Figure 7j). Overall, this reprogramming could enable the robust activation of cytotoxic T cells, ultimately leading to the inhibition of tumor growth (Figure 7k).

Discussion

CRPC exhibits resistance to ADT, and while certain chemotherapeutic agents display effectiveness against CRPC, they are often associated with pronounced systemic adverse effects.[32] Conventional immunotherapy may be ineffective against PCa due to the immunosuppressive tumor microenvironment and limited immunogenicity. In the CheckMate 650 study, only 3 out of 30 mCRPC patients, previously treated with endocrine therapy and chemotherapy, exhibited objective responses to targeting anti-PD-1 with anti-CTLA-4 therapy.[33] The success of Sipuleucel-T demonstrates that DC-based immunotherapy is practical, safe, and capable of inducing or enhancing tumor-specific immune responses. Nevertheless, the short prolongation of recipient lives demonstrates the unsatisfactory outcomes of PCa patients and the need for more effective therapeutics.[5]

Successful translational research depends on appropriate animal models. The expression of classic prostate TAAs in the normal tissues of C57BL/6 mice is similar to their expression in humans, based on publicly available mass spectrometry data.[21] The expression levels of the four TAAs chosen in this study were verified in the RM-1-PSMA cell line used in our murine homograft tumor model. CV9103 and CV9104 are PCa TAA-based mRNA therapeutics. However, although these TAA-based mRNA therapies can stimulate patient-specific immunity in prostate cancer, they have not achieved satisfactory results in clinical trials.[4] The specific immunogenicity of the chosen TAAs in this study was verified by ELISpot in mice. Unexpectedly, compared with single TAA mRNA-LNPs monotherapy, the combined treatment with four TAAs did not prolong the overall survival of RM-1-PSMA C57BL/6 model mice. This result indicates that in the prostate cancer mouse model, simply increasing the amount of TAA mRNA cannot effectively improve the outcome of tumor-bearing mice, suggesting that we need to use adjuvant or other means to improve the outcome of tumor-bearing mice. However, considering the coverage of TAAs in clinical prostate cancers and the confirmed immune response activation induced by all four selected TAAs, we used all four TAA mRNA-LNPs (Tetra) in our subsequent study.

Brenda et al. utilized electroporation technology to introduce mRNA encoding CD70, CD40L, and TLR4 into DCs, and demonstrated that it could significantly promote T cell activation in vivo.[34] On this basis, we devised and validated the proficiency of lipid nanoparticles as carriers for mRNA delivery to lymph nodes. This strategy aims to transfect DCs, promoting T cell activation and inhibiting tumor growth. ImmunER, including 4-1BBL, OX40L and CCR7, was successfully constructed and evaluated in two classical animal models. In a B16-OVA murine model, 2/7 mice reached CR and the tumors were under 100 mm^3 in more than half the mice after OVA and ImmunER treatment. In a TC-1 murine model, 10/12 mice achieved CR. Subsequently, we observed that ImmunER increased the proportion of OVA-peptide-presenting DCs in lymph nodes, augmented the percentage of OVA-specific T cells in both spleen and tumor tissues, heightened the secretion of IFN-γ by T cells, and bolstered the presence of memory T cells in the blood. Adaptive immunity requires time to initiate; in vivo cell killing assays revealed that ImmunER may activate innate immune cells, prompting them to eliminate extraneous cells.

CD8$^+$ (a) and CD4$^+$T (b) cells in tumor-infiltrating CD3$^+$T cells. (c) Representative flow dot plots and statistical analysis of CD8$^+$4-1BB$^+$T cells in the tumor. (d) Representative flow dot plots and statistical analysis of CD8$^+$OX40$^+$T cells in the tumor. (e) Representative flow dot plots and statistical analysis of CD8$^+$CD44$^+$T cells in the tumor. (f and g) The percentages of Tregs (f) and TCM (g) in CD4$^+$T cells from spleen. (h and i) The percentages of perforin-positive (h) and granzyme B-positive (i) cells in CD8$^+$T cells from spleen. (j) The percentages of TCM in CD8$^+$T cells from spleen. Data in a to j were presented as means ± SEM. Statistical significance was determined by One-Way ANOVA (a to j). *$P < .05$, **$P < .01$, ***$P < .001$, and ****$p < .0001$.
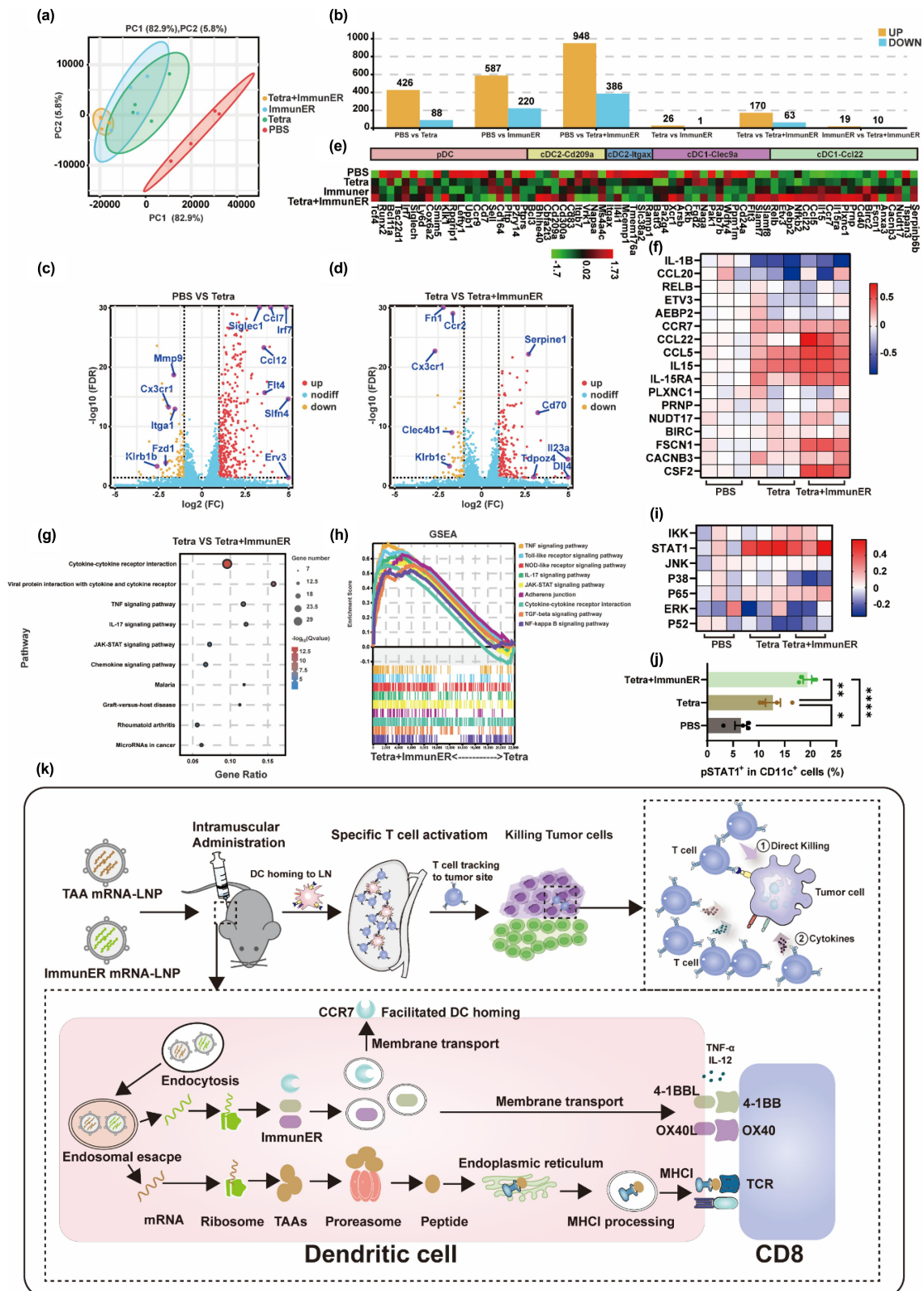
Figure 7. Sequencing of mRNA reveals the upregulation of cDC1-Ccl22 related genes and STAT1. BMDCs (day 6, n = 4) transfected with 1 μg/ml different mRNA-LNPs for 24 h were lysed with Trizol and sent for mRNA sequencing. (a) Principal component analysis revealed that mRNA-LNPs-treated BMDCs formed separate clusters from the control mice group. (b) Statistical analysis of differentially expressed genes between the BMDC groups treated with different mRNA-LNPs. (c and d) Volcano plots showing the 514 (PBS vs. Tetra) (c) and 233 (Tetra vs. Tetra + ImmunER) (D) differentially expressed genes identified by RNA sequencing (p < .05) with a fold change greater than or equal to 2.0. (e) A heatmap showing the expression of genes associated with the DC subset. (f) The differential expression levels of 17 cDC1-CCL22-related genes were confirmed by qPCR (n = 3). (g and h) KEGG enrichment analysis (g) and GSEA (h) in the Tetra + ImmunER vs. Tetra groups. (i) The differential expression levels of pathway-related genes were confirmed by qPCR (n = 3). (j) Flow cytometry analysis showed the expression of pSTAT1 in BMDCs. (k) Diagram illustrated the strategy of intramuscular administration of Tetra and ImmunER to effectively stimulate T cells for the treatment of prostate cancer. Data in j were presented as means ± SEM. Statistical significance was determined by One-Way ANOVA (j). *P < .05, **P < .01, and ****p < .0001.

Prostate malignancy is commonly characterized as an immune desert, and the transformation of immunologically cold tumors into a more inflamed state holds promise for improving the outcome of patients with PCa.[35] An RNA seq analysis of BMDCs revealed that ImmunER, when combined with Tetra, significantly upregulated the expression of cDC1-Ccl22 related genes and activated the JAK-STAT signaling pathway. This molecular insight suggests a potential mechanism for the observed therapeutic effects. Flow cytometry results further underscore the capacity of ImmunER to enhance the activation of T cells by DC. The combination of Tetra and ImmunER exhibited superior anti-tumoral effects in a PCa murine model. In the RM-1-PSMA subcutaneous allograft model, three mice treated with this combination therapy survived nearly twice as long as those in the control group. Similarly, in the orthotopic prostate cancer model, mRNA vaccines significantly inhibited tumor proliferation. The RM-1 cell line is insensitive to ICI treatment.[36] However, combining mRNA vaccines with ICI resulted in 2/5 PCa-bearing mice achieving CR. ImmunER exhibits the potential to transform the "cold tumor" paradigm by augmenting the accumulation of CD8$^+$T cells, particularly 4-1BB$^+$CD8$^+$T cells and OX40$^+$CD8$^+$T cells, to suppress tumor growth. ImmunER not only augments T cell activation but also enhances the capacity of T cells to produce key immunomodulatory cytokines, such as IFN-γ and TNF-α, within the tumor-suppressive microenvironment of the murine PCa model. Furthermore, in addition to the specific cytotoxicity initiated by the combination therapy with ImmunER and Tetra, humoral immunity was also enhanced.

This paper has some limitations. Firstly, our examination of ImmunER-induced elevation of specific T cells was confined to the B16-OVA animal model. Secondly, we evaluated the mRNA vaccine using only one PCa cell line. Furthermore, the underlying molecular mechanisms of ImmunER necessitate further exploration. Despite these limitations, we believe that these constraints do not undermine the integrity or validity of our conclusions.

In summary, we demonstrated the efficacy of a combinatorial mRNA-LNPs-based approach that includes PCa Tetra (PAP, PSCA, PSMA, TGM4 mRNA-LNPs) and ImmunER (4-1BBL, OX40L, CCR7 mRNA-LNPs) to enhance specific T cell cytotoxicity required for tumor elimination. In addition, the safety evaluation revealed that the treatment regimen did not damage normal tissues. This study is an essential first step in facilitating the clinical application of mRNA-LNPs-based therapy in patients with PCa.

Acknowledgments

Disclosure statement

The lipid A1A3 is described in a Chinese patent CN114105799B. ZGF is the inventor of patent application CN114105799B, which covers a method for the synthesis of cationic lipids. The remaining authors declare that they have no competing interests.

Funding

ORCID

Jun Pang http://orcid.org/0000-0003-0024-9415

Author contribution

Conceptualization and Supervision: PJ, ZGF
Methodology: XZX, XZ
Investigation: XZ, WJ, XZX, QHW, ZSQ
mRNA and therapeutic production: XZ, WJ, XH, HYR
Animal model establishment: XZ, WJ, QHW, ZSQ, XYD
Cell experiments: XZ, WJ, CF, LHQ
Data analysis and interpretation: XZ, WJ, XZX
Writing: XZ, XZX

Data and materials availability

All experimental data associated with this study are present in the paper or the supplementary materials. Raw RNA-seq data were deposited to the National Center for Biotechnology Information Sequence Read Archive (NCBI) (https://trace.ncbi.nlm.nih.gov/Traces/sra) under accession number PRJNA1009387.

References

1. Miller KD, Nogueira L, Devasia T, Mariotto AB, Yabroff KR, Jemal A, Kramer J, Siegel RL. Cancer treatment and survivorship statistics, 2022. CA Cancer J Clin. 2022 Sep;72(5):409–436. doi:10.3322/caac.21731.

2. Cheng Q, Butler W, Zhou Y, Zhang H, Tang L, Perkinson K, Chen X, Jiang X, McCall SJ, Inman BA, et al. Pre-existing castration-resistant prostate cancer–like cells in primary prostate cancer promote resistance to hormonal therapy. Eur Urol. 2022 May;81(5):446–455. doi:10.1016/j.eururo.2021.12.039.

3. Bright RK, Bright JD, Byrne JA. Overexpressed oncogenic tumor-self antigens. Hum Vaccin Immunother. 2014;10(11):3297–3305. doi:10.4161/hv.29475.

4. Rausch S, Schwentner C, Stenzl A, Bedke J. mRNA vaccine CV9103 and CV9104 for the treatment of prostate cancer. Hum Vaccin Immunother. 2014;10(11):3146–3152. doi:10.4161/hv.29553.

5. Kantoff PW, Higano CS, Shore ND, Berger ER, Small EJ, Penson DF, Redfern CH, Ferrari AC, Dreicer R, Sims RB, et al. Sipuleucel-T immunotherapy for castration-resistant prostate cancer. N Engl J Med. 2010 Jul 29;363(5):411–422. doi:10.1056/NEJMoa1001294.

6. Sartor O, de Bono J, Chi KN, Fizazi K, Herrmann K, Rahbar K, Tagawa ST, Nordquist LT, Vaishampayan N, El-Haddad G, et al. Lutetium-177–PSMA-617 for metastatic castration-resistant prostate cancer. N Engl J Med. 2021 Sep 16;385(12):1091–1103. doi:10.1056/NEJMoa2107322.

7. Lopez-Bujanda ZA, Obradovic A, Nirschl TR, Crowley L, Macedo R, Papachristodoulou A, O'Donnell T, Laserson U, Zarif JC, Reshef R, et al. TGM4: an immunogenic prostate-restricted antigen. J Immunother Cancer. 2021 June;9(6):e001649. doi:10.1136/jitc-2020-001649.

8. Miao L, Li L, Huang Y, Delcassian D, Chahal J, Han J, Shi Y, Sadtler K, Gao W, Lin J, et al. Delivery of mRNA vaccines with heterocyclic lipids increases anti-tumor efficacy by

STING-mediated immune cell activation. Nat Biotechnol. 2019 Oct;37(10):1174–1185. doi:10.1038/s41587-019-0247-3.

9. Wculek SK, Cueto FJ, Mujal AM, Melero I, Krummel MF, Sancho D. Dendritic cells in cancer immunology and immunotherapy. Nat Rev Immunol. 2020 Jan;20(1):7–24. doi:10.1038/s41577-019-0210-z.

10. Sahin U, Oehm P, Derhovanessian E, Jabulowsky RA, Vormehr M, Gold M, Maurus D, Schwarck-Kokarakis D, Kuhn AN, Omokoko T, et al. An RNA vaccine drives immunity in checkpoint-inhibitor-treated melanoma. Nature. 2020 Sep;585 (7823):107–112. doi:10.1038/s41586-020-2537-9.

11. Paston SJ, Brentville VA, Symonds P, Durrant LG. Cancer vaccines, adjuvants, and delivery systems. Front Immunol. 2021;12:627932. doi:10.3389/fimmu.2021.627932.

12. Marciscano AE, Anandasabapathy N. The role of dendritic cells in cancer and anti-tumor immunity. Semin Immunol. 2021 Feb;52:101481. doi:10.1016/j.smim.2021.101481.

13. Brandum EP, Jørgensen AS, Rosenkilde MM, Hjortø GM. Dendritic cells and CCR7 expression: an important factor for autoimmune diseases, chronic inflammation, and cancer. Int J Mol Sci. 2021 Aug 3;22(15):8340. doi:10.3390/ijms22158340.

14. Salem A, Alotaibi M, Mroueh R, Basheer HA, Afarinkia K. CCR7 as a therapeutic target in cancer. Biochim Biophys Acta Rev Cancer. 2021 Jan;1875(1):188499. doi:10.1016/j.bbcan.2020.188499.

15. Wang C, Lin GH, McPherson AJ, Watts TH. Immune regulation by 4-1BB and 4-1BBL: complexities and challenges. Immunological Rev. 2009 May;229(1):192–215. doi:10.1111/j.1600-065X.2009.00765.x.

16. Fu Y, Lin Q, Zhang Z, Zhang L. Therapeutic strategies for the costimulatory molecule OX40 in T-cell-mediated immunity. Acta Pharm Sin B. 2020;10(3):414–433. doi:10.1016/j.apsb.2019.08.010.

17. Hotz C, Wagenaar TR, Gieseke F, Bangari DS, Callahan M, Cao H, Diekmann J, Diken M, Grunwitz C, Hebert A, et al. Local delivery of mRNA-encoded cytokines promotes antitumor immunity and tumor eradication across multiple preclinical tumor models. Sci Transl Med. 2021 Sep 8;13(610):eabc7804. doi:10.1126/scitranslmed.abc7804.

18. Fromm G, de Silva S, Giffin L, Xu X, Rose J, Schreiber TH. Gp96-Ig /Costimulator (OX40L, ICOSL, or 4-1BBL) combination vaccine improves T-cell priming and enhances immunity, memory, and tumor elimination. Cancer Immunol Res. 2016 Sep 2;4(9):766–778. doi:10.1158/2326-6066.CIR-15-0228.

19. Xu Y, Hu Y, Xia H, Zhang S, Lei H, Yan B, Xiao ZX, Chen J, Pang J, Zha G-F. Delivery of mRNA vaccine with 1, 2-diesters-derived lipids elicits fast liver clearance for safe and effective cancer immunotherapy. Adv Healthc Mater. 2023 Nov 21;13(5): e2302691. doi:10.1002/adhm.202302691.

20. Sauter M, Sauter RJ, Nording H, Olbrich M, Emschermann F, Langer HF. Protocol to isolate and analyze mouse bone marrow derived dendritic cells (BMDC). STAR Protoc. 2022 Sep 16;3 (3):101664. doi:10.1016/j.xpro.2022.101664.

21. Lu T, Qian L, Xie Y, Zhang Q, Liu W, Ge W, Zhu Y, Ma L, Zhang C, Guo T, et al. Tissue-characteristic expression of mouse proteome. Mole Cell Proteomics: MCP. 2022 Oct;21(10):100408. doi:10.1016/j.mcpro.2022.100408.

22. Zhuang X, Qi Y, Wang M, Yu N, Nan F, Zhang H, Tian M, Li C, Lu H, Jin N. mRNA vaccines encoding the HA protein of influenza a H1N1 virus delivered by cationic lipid nanoparticles induce protective immune responses in mice. Vaccines (Basel). 2020 Mar 10;8(1):123. doi:10.3390/vaccines8010123.

23. Xu J, Lv J, Zhuang Q, Yang Z, Cao Z, Xu L, Pei P, Wang C, Wu H, Dong Z, et al. A general strategy towards personalized nanovaccines based on fluoropolymers for post-surgical cancer immunotherapy. Nat Nanotechnol. 2020 Dec;15(12):1043–1052. doi:10.1038/s41565-020-00781-4.

24. Bedoui S, Whitney PG, Waithman J, Eidsmo L, Wakim L, Caminschi I, Allan RS, Wojtasiak M, Shortman K, Carbone FR, et al. Cross-presentation of viral and self antigens by skin-derived CD103+ dendritic cells. Nat Immunol. 2009 May;10(5):488–495. doi:10.1038/ni.1724.

25. Slavin-Chiorini DC, Catalfamo M, Kudo-Saito C, Hodge JW, Schlom J, Sabzevari H. Amplification of the lytic potential of effector/memory CD8+ cells by vector-based enhancement of ICAM-1 (CD54) in target cells: implications for intratumoral vaccine therapy. Cancer Gene Ther. 2004 Oct;11(10):665–680. doi:10.1038/sj.cgt.7700741.

26. Saxena M, van der Burg SH, Melief CJM, Bhardwaj N, van der Burg SH. Therapeutic cancer vaccines. Nat Rev Cancer. 2021 June;21(6):360–378. doi:10.1038/s41568-021-00346-0.

27. Brina D, Ponzoni A, Troiani M, Calì B, Pasquini E, Attanasio G, Mosole S, Mirenda M, D'Ambrosio M, Colucci M, et al. The Akt/mTOR and MNK/eIF4E pathways rewire the prostate cancer translatome to secrete HGF, SPP1 and BGN and recruit suppressive myeloid cells. Nat Cancer. 2023 Aug;4(8):1102–1121. doi:10.1038/s43018-023-00594-z.

28. Liu Q, Sun Z, Chen L. Memory T cells: strategies for optimizing tumor immunotherapy. Protein Cell. 2020 Aug;11(8):549–564. doi:10.1007/s13238-020-00707-9.

29. Voskoboinik I, Whisstock JC, Trapani JA. Perforin and granzymes: function, dysfunction and human pathology. Nat Rev Immunol. 2015 Jun;15(6):388–400. doi:10.1038/nri3839.

30. Zhang L, Li Z, Skrzypczynska KM, Fang Q, Zhang W, O'Brien SA, He Y, Wang L, Zhang Q, Kim A, et al. Single-cell analyses inform mechanisms of myeloid-targeted therapies in colon cancer. Cell Apr. 2020 16;181(2):442–459.e29. doi:10.1016/j.cell.2020.03.048.

31. Zhao H, Wu L, Yan G, Chen Y, Zhou M, Wu Y, Li Y. Inflammation and tumor progression: signaling pathways and targeted intervention. Sig Transduct Target Ther. 2021 Jul 12;6(1):263. doi:10.1038/s41392-021-00658-5.

32. Teo MY, Rathkopf DE, Kantoff P. Treatment of advanced prostate cancer. Annu Rev Med. 2019 Jan 27;70(1):479–499. doi:10.1146/annurev-med-051517-011947.

33. Sharma P, Pachynski RK, Narayan V, Fléchon A, Gravis G, Galsky MD, Mahammedi H, Patnaik A, Subudhi SK, Ciprotti M, et al. Nivolumab plus ipilimumab for metastatic castration-resistant prostate cancer: preliminary analysis of patients in the CheckMate 650 Trial. Cancer Cell. 2020 Oct 12;38 (4):489–499.e3. doi:10.1016/j.ccell.2020.08.007.

34. Van Lint S, Renmans D, Broos K, Goethals L, Maenhout S, Benteyn D, Goyvaerts C, Du Four S, Van der Jeught K, Bialkowski L, et al. Intratumoral delivery of TriMix mRNA results in T-cell activation by cross-presenting dendritic cells. Cancer Immunol Res. 2016 Feb;4(2):146–156. doi:10.1158/2326-6066.CIR-15-0163.

35. Fizazi K, Drake CG, Beer TM, Kwon ED, Scher HI, Gerritsen WR, Bossi A, den Eertwegh AJMV, Krainer M, Houede N, et al. Final analysis of the ipilimumab versus placebo following radiotherapy Phase III trial in postdocetaxel metastatic castration-resistant prostate cancer identifies an excess of long-term survivors. Eur Urol. 2020 Dec;78(6):822–830. doi:10.1016/j.eururo.2020.07.032.

36. Allard B, Pommey S, Smyth MJ, Stagg J. Targeting CD73 enhances the antitumor activity of anti-PD-1 and anti-CTLA-4 mAbs. Clin Cancer Res. 2013 Oct 15;19(20):5626–5635. doi:10.1158/1078-0432.CCR-13-0545.